Theoretical and Applied Climatology (2021) 143:1–18
https://doi.org/10.1007/s00704-020-03379-x

ORIGINAL PAPER

Will the wind associated with the Adriatic storm surges change in future climate?

Iva Međugorac[1] · Mira Pasarić[1] · Ivan Güttler[2]

Received: 8 May 2020 / Accepted: 11 September 2020 / Published online: 21 September 2020

Abstract

Flooding of the Adriatic coastline is predominantly caused by storm surges induced by winds from the south-eastern sector. This phenomenon in Venice is known as *acqua alta*. We present a study of wind fields favouring storm-surge setups in the Adriatic, including their characteristics in the present climate and their expected characteristics in future scenarios. Analysis is based on (i) measured sea levels in Venice and Bakar (1984–2014), (ii) near-surface wind from ERA5 reanalysis, and (iii) simulations of wind fields with three regional climate models (ALADIN52, RCA4, and RegCM4) forced with several global models (CNRM-CM, MPI-ESM-MR/LR, HadGEM2-ES, EC-EARTH, and IPSL-CM5). For future climates, we considered two scenarios (RCP4.5 and RCP8.5) and two future periods (2041–2070 and 2071–2100) with respect to the historical 1971–2000 period. It was found that the probability that the frequency, intensity, annual cycle, and spatial structure of the wind inducing the Adriatic storm surges will change in future climates is small. The result is robust and consistent according to all considered criteria—it does not depend on the analysed regional climate models, boundary conditions, climate scenarios, or future time interval.

1 Introduction

The Adriatic is the Mediterranean sub-basin surrounded by mountains. Its elongated shape, shallow closed end (< 50 m), and surrounding orography support atmospheric fields that give rise to storm surges that occasionally flood the coastline. Flooding occurs mostly in late autumn and during winter when the Mediterranean cyclones travel over the Adriatic, inducing an air pressure gradient and southeasterly wind (*Sirocco*). Both the meteorological forcings act in the same sense—they cause water to accumulate at the closed end of the basin, endangering many coastal cities (Robinson et al. 1973; Trigo and Davies 2002). The most vulnerable city is Venice, a city of great historical and cultural heritage, situated at the end of the longest *Sirocco* fetch and lying on the low-level ground. Significant effort has been engaged in order to model and predict storm-surge induced coastal flooding in the Adriatic, with the focus on the Venice lagoon (e.g. Bajo et al. 2007; Bajo and Umgiesser 2010; Bajo et al. 2019). However, cities south of Venice can also be considerably endangered by high water regimes. In the last 15 years, several intense events occurred, affecting the eastern coast in particular. At the Croatian station Bakar, operating since 1929, the absolute sea-level maximum was repeatedly surpassed on 1 December 2008, 23 and 25 December 2009, 1 December 2012, 29 October 2018, and 13 November 2019. On these occasions, the sea level surpassed the highest level ever observed previously at this station (Međugorac et al. 2015, 2016; AMGI 2018). The increasing number of eastern Adriatic floods in the last decades has motivated researchers to examine meteorological conditions under which storm surges develop with distinct impact along one of the two opposite coasts (Međugorac et al. 2018). Under certain atmospheric conditions, a cross-basin sea-level slope (i.e. transverse sea-level slope, TSLS) is established, which results in stronger flooding of a particular coastline. The study, based on a 31-

Electronic supplementary material The online version of this article (https://doi.org/10.1007/s00704-020-03379-x) contains supplementary material, which is available to authorized users.

✉ Iva Međugorac
ivamed@gfz.hr

Mira Pasarić
mpasaric@gfz.hr

Ivan Güttler
ivan.guettler@cirus.dhz.hr

[1] Department of Geophysics, Faculty of Science, University of Zagreb, Horvatovac 95, 10000 Zagreb, Croatia

[2] Croatian Meteorological and Hydrological Service, Grič 3, 10000 Zagreb, Croatia

year-long series (1984–2014) of sea level (Bakar and Venice) and atmospheric fields (ERA-Interim, Dee et al. 2011), classified storm surges according to their TSLSs: O type (ordinary type of storm surges with a usual TSLS), W type (storm surges with a strong westward slope), and E type (storm surges with an eastward slope). The W type of storm surge is induced by the wind field with *Bora* (north-easterly wind) over the northern part of the Adriatic and uniform *Sirocco* above the rest of the basin. The E type is caused by deeper Mediterranean cyclones shifted to the north, accompanied by wind fields with the following features: a pronounced cross-basin (i.e. transverse, T) component towards the eastern shore and a shear of along-basin (i.e. longitudinal, L) component with higher velocities at the eastern coastline.

In addition to storm surges, several other sea-level processes may support the Adriatic floods and their role depends on their amplitude and phase relative to the storm surge. Tide, pre-existing seiche, and low-frequency (planetary) sea-level variability can considerably raise the height of water if they constructively overlap with the storm surge (Pasarić and Orlić 2001). Amplitudes of all of the involved processes are small in comparison with the basin depth, and their nonlinear interactions are negligible (Vilibić et al. 2017).

The tide in the Adriatic is of a mixed type and traditionally modelled as a superposition of seven major constituents (K1, O1, P1, K2, S2, M2, and N2; Janeković and Kuzmić 2005). The tidal range increases towards the shallow north end, where it comes to approximately 150 cm.

The Adriatic oscillates at several eigenmodes, where the lowest three are at periods of 21.2 h, 10.7 h, and 6.7 h (Cerovečki et al. 1997; Raicich et al. 1999). The first mode (21.2 h) is the most energetic and the most studied one. It is generated by wind transients—when *Sirocco* suddenly ceases or switches to *Bora*. The seiche amplitude increases along the main axis of the basin, reaching its maximum in front of Venice where it can surpass 50 cm (Godin and Trotti 1975). Due to a very long decay period (3.2 ± 0.5 days, Cerovečki et al. 1997), once triggered, it can last for days and take part in upcoming events by mitigating or reinforcing the newly induced storm surge.

The planetary sea-level component is a process that takes place on longer temporal scales, over periods of 10–100 days. This component is dominantly controlled by atmospheric planetary waves, which are prominent in middle and upper layers of the troposphere (Orlić 1983). Planetary waves are seen as waveforms on the 500-hPa geopotential with wavelengths of 6000 to 8000 km. They are most energetic during the cold season when atmosphere is barotropic (Pasarić and Orlić 1992). In these conditions, a disturbance from the middle troposphere is observed undistorted in sea-surface air pressure. This is true in a statistical sense, but it may not be valid in individual cases when the atmosphere is baroclinic or when other low-frequency processes, like thermohaline variability, may have impact on the planetary sea-level component. The low-frequency air pressure and the related wind forcing can induce changes of sea level up to 70 cm in the northern Adriatic (Pasarić and Orlić 1992; Pasarić et al. 2000). The planetary sea-level variability provides strong and days-long preconditions for flooding; it is not the dominant part, but is the ever-present component of the Adriatic coastal floods (Pasarić and Orlić 2001).

The meteorologically driven components of the Adriatic floods may be subject to the impact of climate change. An important question is how expected changes in climate will be reflected in the dominating process, i.e. the storm surge, or more specifically on the atmospheric disturbances controlling it. Few studies have already addressed some aspects of this question, although some of them had mainly methodological goals. Marcos et al. (2011) showed that the frequency and magnitude of storm surges in the Mediterranean Sea will decrease in the twenty-first century (assuming climate scenarios A2, A1B, and B1). Lionello et al. (2012b) found that there is no evidence for more extreme storm surges under future scenarios (B2 and A2). Mel et al. (2013) showed that under the moderate emission scenario (RCP4.5) albeit with certain modified statistics, the frequency of storm surges will not change. Denamiel et al. (2020) found that under conditions of changed climate (RCP4.5 and RCP8.5), twelve storm-surge events observed during 1979–2019 would achieve a lower intensity. However, these results were obtained using a single oceanographic model (HAMSON, HYPSE, or NEMO) forced with a single combination of atmospheric regional–global climate model (ARPEGE-v3, RegCM, EC-Earth, IPSL) and thus are easily biassed and not subjected to statistical evaluation. Evidently, there is a need for comprehensive study of storm surges under future scenarios based on an ensemble of simulations produced with various climate models taking boundary and initial conditions from different sources. The established connection between atmospheric forcing and storm surges (Međugorac et al. 2018) provides means to evaluate properties of storm surges in the Adriatic by analysing results of atmospheric models, which are more readily available than simulations by using oceanographic models. Considering wind as the driving force, this study will focus on properties of the wind fields only.

Risk from storm surges will likely increase in the future due to the rise of the mean sea level, which is expected to be 40–60 cm worldwide by the end of the twenty-first century (IPCC 2013). Therefore, properties of storminess in upcoming decades are a major environmental concern for the Adriatic coastal cities. Important questions are whether the conditions favouring flooding will be more frequent, with what intensity and ultimately which type of conditions will prevail—the one inducing stronger sea-level setup at the eastern coast (E type) or on the opposite side of the Adriatic (W type).

The goals of this study are (i) to evaluate performance of selected regional climate models in reproduction of the wind regimes which generate and control the Adriatic storm surges

and (ii) to investigate the impact of climate change on these wind regimes. Analysis was conducted using sea-level measurements in Venice and Bakar, using simulations of three CORDEX (Jacob et al. 2014; Kotlarski et al. 2014; Ruti et al. 2016) regional climate models (RCMs) forced with several CMIP5 (Taylor et al. 2012) global climate models (GCMs), and considering two future representative concentration pathways (RCP, Moss et al. 2010). In this study, we extend into the future the relationship between storm surges in the Adriatic and their meteorological conditions during the past 31-year period.

The strategy adopted is as follows. Sea level measured at the two northern Adriatic stations and ERA5 reanalysis fields were used to define the detection algorithms that successfully recognised wind structures responsible for the highest storm surges established in the northern Adriatic. The constructed algorithms were then applied to simulations with RCMs in evaluation, historical, and future periods. Performance of the applied RCMs was assessed by comparing statistical properties of the extracted sea-level episodes and the extracted wind episodes. The impact of climate change on wind fields associated with the Adriatic storm surges was determined by comparing the intensity, frequency, seasonal cycle, and type of the wind fields in historical and future periods.

This paper is organised as follows. In Sect. 2, we describe datasets of meteorological simulations and measured sea level, as well as the applied statistical methods. The analysis strategy, adjustment of numerical algorithms, and definitions of wind and sea-level episodes and their types are given in Sect. 3. The results are presented in Sect. 4 and discussed in Sect. 5. We conclude with a brief summary and recommendations for future studies in Sect. 6.

2 Datasets and statistical methods

The data analysis is based on measured sea levels at tide gauge stations in Venice (Punta della Salute) and Bakar (northern Adriatic), and simulated near-surface wind fields were used (Table 1).

Detided sea levels were obtained by subtracting the tidal signal from the total sea level. The tide was calculated using the T_tide tool (Pawlowicz et al. 2002) considering seven major constituents important in the Adriatic (K1, O1, P1, K2, S2, M2) in the period of 1984–2014.

Wind was analysed using four different datasets: ERA5 reanalysis (C3S 2017; Hersbach and Dee 2016; Hersbach et al. 2018; Hersbach et al. 2019) and simulations of three RCMs—ALADIN52 (Colin et al. 2010), RCA4 (Samuelsson et al. 2011), and RegCM4 (Giorgi et al. 2012). The three RCMs were chosen due to availability of subdaily fields. Wind fields from ERA5, with spatial resolution approximately 30 km above the Adriatic, were resampled to 6-h intervals, as well as the RCM winds, for all simulations, to achieve the same temporal resolution for all datasets. The spatial resolution of the data produced with RCMs was 12.5 km. RCA4 and RegCM4 simulations were carried out according to the EURO-CORDEX protocol (Jacob et al. 2014; Kotlarski et al. 2014), while simulations with ALADIN52 were done via the Med-CORDEX protocol (Ruti et al. 2016). The main difference between the analysed RCM simulations was in domain size: the whole of Europe in EURO-CORDEX and the broader Mediterranean area in Med-CORDEX. Initial and boundary conditions for simulations with three RCMs were taken from CMIP5 global models (Taylor et al. 2012): (1) CNRM-CM, (2) MPI-ESM-MR/LR, (3) HadGEM2-ES, (4) EC-EARTH, and (5) IPSL-CM5. For ALADIN52, only simulations forced with global model (1) were available. For RCA4, simulations with global models (1)–(5) were available, while for RegCM4, simulations with global models (1)–(4) were available. Wind fields were analysed according to their availability: a time interval of 1971–2070 for RegCM4 and 1971–2099/2100 for the other two models. Simulations until the year 2000 were carried out using observed greenhouse gas concentrations, while those after 2000 were performed using two climate scenarios: RCP4.5 and RCP8.5 (Moss et al. 2010).

The statistical significance of differences between future and present wind characteristics was determined by using the Wilcoxon–Mann–Whitney rank-sum test (WMW, Fisz 1963). This is a non-parametric statistical test used for variables without normal distributions. The information obtained with the WMW test was supplemented with the probability density function (PDF)–based climate change measure $PCC = 1\text{-}PSS$, where PSS is the *Perkins skill score* (Perkins et al. 2007). PSS is a probability density function–based measure, defined by the relation

$$PSS = \sum_{1}^{n} \min\left(Z_h, Z_p\right), \tag{1}$$

where n is the number of bins used to calculate the PDF of a simulation, and Z_h and Z_p are the frequency of values in a given bin for a historical period and for a projection, respectively. This metric measures similarity between two PDFs, i.e. measures common area between the two distributions. If the two PDFs negligibly overlap (i.e. they are clearly distinct), then the *Perkins skill score* is close to zero and PCC is close to one (Belušić Vozila et al. 2019). In this study, we divided PCC into three categories: small ($0 \le PCC < 0.3$), moderate ($0.3 \le PCC < 0.6$), and high ($0.6 \le PCC \le 1.0$) probability of climate change.

3 Formulation of algorithms for the extraction of flood episodes

The first step in the analysis was to create algorithms that would extract from the meteorological database those meteorological situations that are truly responsible for the observed floods. For this purpose, it was necessary to consider wind fields that are

Table 1 Sea-level series and wind fields from different datasets. The first column shows used data: measured sea level and wind from reanalysis and simulations carried out with three regional climate models forced with different global climate models. Data are available for intervals listed in columns 2–4, while temporal and spatial resolution of the data series are given in the last two columns

Data/models	Measurements/reanalysis/ evaluation	Historical period	Projections CP4.5/RCP8.5	Temporal resolutions (hour)	Spatial resolution (km)
Sea level (Venice/Bakar)	1984–2014			1	
ERA5	1984–2014			3	~30
ALADIN52 CNRM-CM5	1984–2012	1971–2000	2041–2100	3	12.5
RCA4					
CNRM-CM5			2041–2100		
MPI-ESM-LR			2041–2099		
HadGEM2-ES	1984–2010	1970–2005	2041–2099	6	12.5
EC-EARTH			2041–2100		
IPSL-CM5			2041–2100		
RegCM4					
CNRM-CM5					
MPI-ESM-MR	1984–2014	1970–2005	2041–2070	3	12.5
HadGEM2-ES					
EC-EARTH					

known to reliably reproduce flow patterns above the Adriatic. We used ERA5 reanalysis, a dataset that replaced ERA-Interim, which, despite a rough resolution in the Adriatic region (approximately 80 km), successfully represents circulation with exceptional temporal correlation (Menendez et al. 2014; Dutour Sikirić et al. 2015; Belušić et al. 2018). However, ERA5 reanalysis is significantly improved with respect to ERA-Interim: the ERA5 winds show much better agreement with satellite-based wind field observations (Belmonte Rivas and Stoffelen 2019) and provide large improvement in storm surge modelling (Dullaart et al. 2020). Moreover, ERA5 successfully detects extreme storm-surge events in the northern Adriatic in terms of sea-level height (Porcu et al. 2020). The higher resolution meteorological forcing dataset is important in the Adriatic, where small spatial changes in wind (e.g. the presence of *Sirocco* shear in the middle Adriatic or *Bora* over the northernmost part of the Adriatic) are manifested in significantly different sea-level responses (E or W type of storm surges; Međugorac et al. 2018).

After the extracting algorithms had been adjusted on ERA5 wind data, the identical procedures were applied to RCM simulations forced by the ERA-Interim reanalysis. In this section, we describe methods used to define: (i) exceptional episodes detected in sea level (sea-level episodes), (ii) exceptional episodes detected from the wind data (wind episodes), and (iii) classified wind episodes (according to the type of flood they cause).

3.1 Extraction of sea-level episodes

Intense sea-level episodes in the northern Adriatic, during the 1984–2014 interval, were singled out using detided sea levels recorded at tide gauge stations in Bakar and Venice. The two series were reduced to the same reference level by subtracting 31-year means from the measurements and taking into account the respective long-term trends. The sea-level trend observed from data measured by the tide gauge is controlled by using processes of different origins. These are changes in direct atmospheric processes (i.e. air pressure and wind), steric changes related to thermohaline processes, and changes of water mass and vertical land movements. To analyse changes in the occurrence and intensity of extreme storm surges over time, we remove the sea-level trend that is induced by using the later three processes, but retain the part due to direct atmospheric forcing. The method and trend analysis are described in more detail in the Appendix. Once the trends of non-meteorological origin were removed from the detided sea levels, exceptional storm surges in the northern Adriatic were identified following the approach introduced in Međugorac et al. (2018). Individual storm surge events were defined as every occurrence of the residual (detided and detrended) sea level (Zr) exceeding a given threshold, at least at one of the stations. The threshold imposed was the 99.95 percentile of the data from both stations (71.84 cm). Subsequent sea levels exceeding the threshold were grouped in one episode with the maximum value taken to represent the episode. Independent episodes were defined as those separated by at least 36 h.

3.2 Extraction of wind episodes

For a definition of intense wind episodes, here, using ERA5 reanalysis and later RCM simulations, conditions on wind speed, duration, and direction were imposed. An episode

was declared intense if the wind field over the Adriatic had the following characteristics: wind from the SE quadrant including a small section of the SW quadrant over 70% of the basin, with an average speed exceeding 10.5 m/s for more than 6 h (Fig. 1, right). Consecutive values were grouped in one episode with a speed that corresponds to the maximum value, where separate events were considered those that were at least 24 h apart. The above criteria were set following the principle that the two datasets, episodes extracted directly from the sea-level data (sea-level episodes) and episodes extracted directly from the wind fields (wind episodes), optimally overlap (Fig. 1, left). More specifically, the parameters were adjusted to obtain the maximum ratio of realised episodes (wind episodes that resulted with extreme sea levels) to unrealised (wind episodes that were not observed in sea level) and nonattributed episodes (episodes of extreme sea level that were not identified by the wind field algorithm).

Behaviour of the episodes' ratio to possible wind velocity and wind duration thresholds was examined by using a sensitivity analysis, as shown in Fig. 2. Several combinations of velocity and its duration proved to be optimal for definition of storm surge–related wind episodes. However, the best result—high ratio of episodes and minimum number of nonattributed sea-level events—was achieved for wind velocity higher than 10.5 m/s that lasted more than 6 h.

A wind episode was declared realised if it occurred 26 h before/after a sea-level episode. This interval was determined after testing a larger set of possible values. For each wind episode, corresponding sea-level contributions to sea-level extremes in Venice and Bakar were estimated. The planetary component (*Zlp*) was determined by applying a low-pass digital filter with the half-power point at 10 days, while the synoptic contribution (*Zr-Zlp*) was defined as the variability of sea level when the planetary component was removed from the residual sea level. The high-frequency (synoptic) component encompassed of storm surge and seiche activity, if previously generated. Values of the two sea-level contributions (*Zlp* and *Zr-Zlp*) were taken at the moment when the residual sea level reached its maximum but not later than 12 h after the wind maximum, thus taking into account the response time of sea level to atmospheric forcing (Orlić et al. 1994).

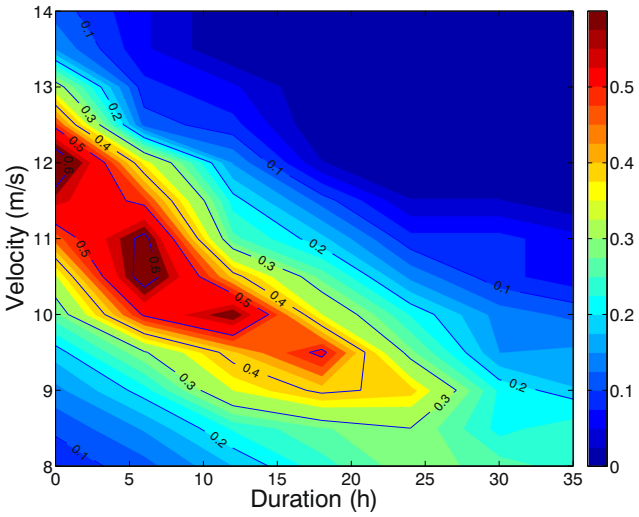

Fig. 2 Ratio of the number of realised wind episodes to the sum of the number of unrealised wind episodes and the number of nonattributed sea-level episodes, depending on a wind velocity threshold (mean velocity over the Adriatic) and its duration

For each event, it was estimated whether it was affected by a previously generated seiche, which could also impact the height of the sea level. The presence of a pre-existing seiche was determined subjectively—by visual inspection of *Zr*, it was established whether it had exhibited sudden changes within a short period (up to 3 days) before the main peak with apparent oscillations afterwards.

3.3 Classification of wind episodes

The extracted wind fields were classified according to their specific effect on the sea level. This is relevant because subtle changes in the wind field generate notably different sea-level responses along the two coastlines, thereby dictating their

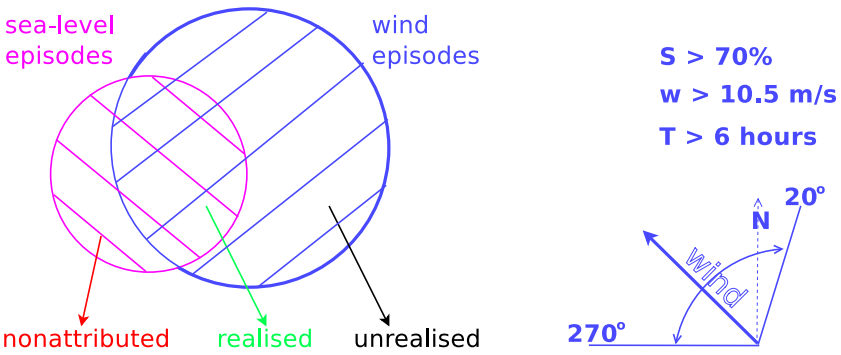

Fig. 1 Left: schematic representation of the procedure for the extraction of wind episodes. Episodes were sorted into three categories—*realised* (observed in both wind and sea-level data), *unrealised* (observed only in wind data), and *nonattributed* (observed only in sea-level data). The procedure was based on optimal overlap of the two datasets, which resulted in the conditions shown on the right. Right: allowed wind directions over at least 70% of the basin surface (*S*) with a minimum velocity of 10.5 m/s (*w*) that lasted more than 6 h (*T*)

exposure to flooding (Međugorac et al. 2018). For the past period, classification was performed using the related cross-basin sea-level slope (TSLS), defined as the difference between the residual sea levels in Venice and Bakar. However, to be able to determine chances of occurrence of storm surges of a certain type in a future climate, based on wind field only, it was necessary to use some other method that would identify the three wind types (W, O, or E). Wind field patterns responsible for the W, O, and E types of storm surges were defined using sea-level episodes and ERA5 fields, following the approach described in Međugorac et al. (2018). Specifically, meteorological backgrounds of each event were identified considering that the current sea state is a reflection of previous atmospheric conditions and taking into account the response time of the sea to synoptic wind forcing, which is about 6 h in the northern Adriatic (Orlić et al. 1994). Thus, the wind fields responsible for storm surges were chosen as those available at least 4 h before the sea level reached its maximum. The constraint of 4 h was obtained experimentally since literature is not extensive on this subject. Then, sea-level episodes and the background wind fields were divided into three categories according to the observed cross-basin sea-level slope: the W and E types were defined as those whose slope deviates from the mean value for more than one standard deviation, while the rest were declared as the O type. For the three storm-surge types, composite wind fields were constructed. The three mean fields were then used as patterns in the detecting phase during which wind fields from the RCM simulations (historical and projections) were classified into one of the characteristic patterns by searching for the minimum Euclidean distance between the established patterns and the given wind field, taking into account only nodes above the Adriatic.

4 Results

4.1 Overview of extracted episodes

According to the proposed procedures, we extracted 39 sea-level and 61 wind episodes in the 1984–2014 interval. The set of wind episodes consisted of 28 realised and 33 unrealised events, extracted from the ERA5 wind field with the help of mareographic data (Fig. 1, left).

It is not surprising that all wind episodes do not manifest as extreme sea levels because the formation of the latter is not a result of the current atmospheric situation alone but also of the preceding atmospheric conditions and the state of the underlying sea. Considering features of the extracted events (Fig. 3), it is evident that, in the realised episodes, wind was generally higher and lasted longer. In addition, the effect of the wind field was superimposed on sea-level variations that are controlled by using processes at different temporal and spatial scales. Therefore, extreme sea levels emerged in episodes where the water level was already elevated due to atmospheric forcing on a planetary scale (high *Zlp*, which was over 30 cm in more than a quarter of all cases). In addition to this, on some occasions, seiche oscillations were already active (marked by crosses in Fig. 3), and depending on relative phases, they further raised or lowered the sea level generated by direct atmospheric forcing. Alternately, almost all of the nonattributed sea-level events were related to small-amplitude wind acting over considerably raised sea level due to planetary processes or oscillations of previously triggered seiches (example in the Supplementary Materials, Fig. S1).

To ascertain that we extracted wind fields that generate sea-level response as observed in the independently extracted episodes of sea level, we compared relative histograms of TSLS for the wind and the sea-level episodes (Fig. 4). It is possible, given the range of permitted wind directions (Fig. 1, right), that we have eliminated certain structures of wind fields that appear above the basin but are relevant for our analysis, and vice versa. The two distributions are similar with the sea-level slopes distributed about the same averages and with similar standard deviations. The differences appear in the presence/absence of certain values—in the wind-based episodes, large positive slopes (approximately 50 cm) are not present, while negative slopes (sea level higher in Bakar) are more frequent.

The background wind fields (Fig. 5) for the three types of storm surges (Fig. 4, left) were used as patterns for classification of RCM fields. The W-type pattern (Fig. 5a) strongly accumulates water near the north-western coastline. It is characterised by almost uniform *Sirocco* above the middle and south Adriatic, while easterly wind dominates over the northernmost part of the basin. The highest wind velocities develop during this type. The O-type pattern (Fig. 5b) causes the ordinary type of storm surges, i.e. those with average TSLS. With respect to the previous pattern, this field is rotated to the east. The E-type wind field (Fig. 5c) causes an equal response of sea level along the two coastlines or somewhat stronger near the eastern shore. This field features (i) a notable T component towards the east above the entire basin, (ii) minimum velocity near the north-western coastline, and (iii) maximum velocities closer to the eastern shore.

The classification of events based on the three wind field patterns shown in Fig. 5, when compared with direct classification by the TSLS (Fig. 4, left), proved to be rather skillful. It attributed 59% of wind fields, associated with 39 sea-level episodes, to the same type as the direct method. Distribution between the types was as expected—most were categorised as O type (61.5%), while the rest were recognised as W (23.1%) or E type (15.4%). The distribution is very close to that obtained by using the direct method: 69.2% (O type), 15.4% (W type), and 15.4% (E type).

4.2 Performance of the RCMs

Strict criteria were applied to validate the three regional climate models: they were tested in terms of how well they

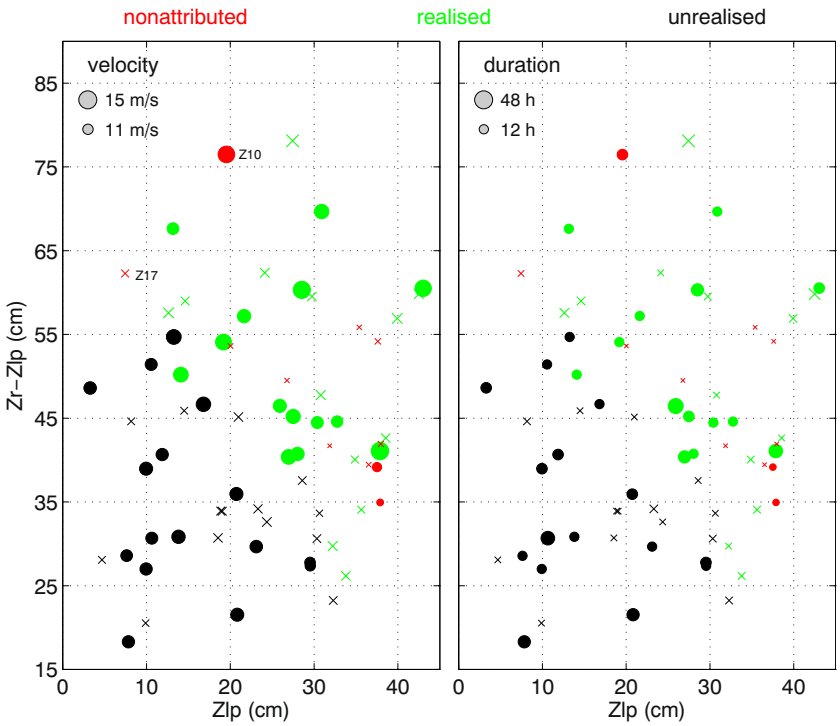

Fig. 3 Planetary (*Zlp*) and synoptic (*Zr-Zlp*) components of the sea level (Venice) for wind and sea-level episodes. The synoptic component represents the joint effect of a storm surge and possible pre-existing seiche. Symbol size indicates the wind velocity (left) or duration (right) of the episode extracted from ERA5. Crosses mark events preceded by seiche oscillations. Nonattributed sea-level episodes Z10 (24 November 1991) and Z17 (28 December 1999) are indicated

reproduce specific meteorological situations using simulations from the evaluation period (run with initial and boundary conditions imposed from ERA-Interim reanalysis). Quality of the modelled fields was assessed considering the total number of extracted wind episodes, as well as the percentage of realised and nonattributed episodes (Table 2). To compare different 1RCMs, we established (i) the same temporal resolution (all fields were resampled to a 6-h interval), (ii) the same spatial resolution (RCM fields were interpolated to the ERA5 grid), and (iii) a common 27-year period from 1984 to 2010. It must be stressed that regional climate models when forced by using the coupled global climate models do not aim to reproduce the actual sequence of, for example, daily/subdaily fields, but only statistics of their variability. However, in the evaluation setup, when forced by the reanalysis that provided boundary and initial conditions for RCM simulations, it is anticipated that models will be able, to some extent, to reproduce actual meteorological situations. Hence, this comparison represents a comprehensive test for the studied RCMs.

Compared with ERA5, the three RCMs yielded a larger number of episodes (Table 2, column 2). This was expected and is due to the better resolution of regional climate models—they develop higher wind velocities and consequently result in a larger number of events that exceed the

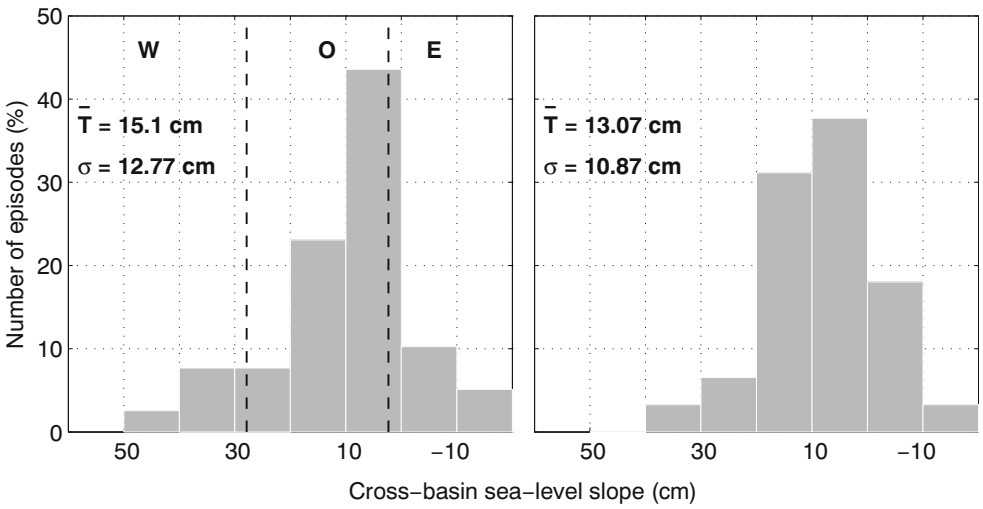

Fig. 4 Distribution of cross-basin sea-level slope (TSLS) for episodes identified from sea-level (left) and ERA5 wind (right) data. Boundaries between the three types (W, O, and E), indicated by vertical lines, are obtained as deviations from the mean value ($\overline{T}$) for one standard deviation (σ)

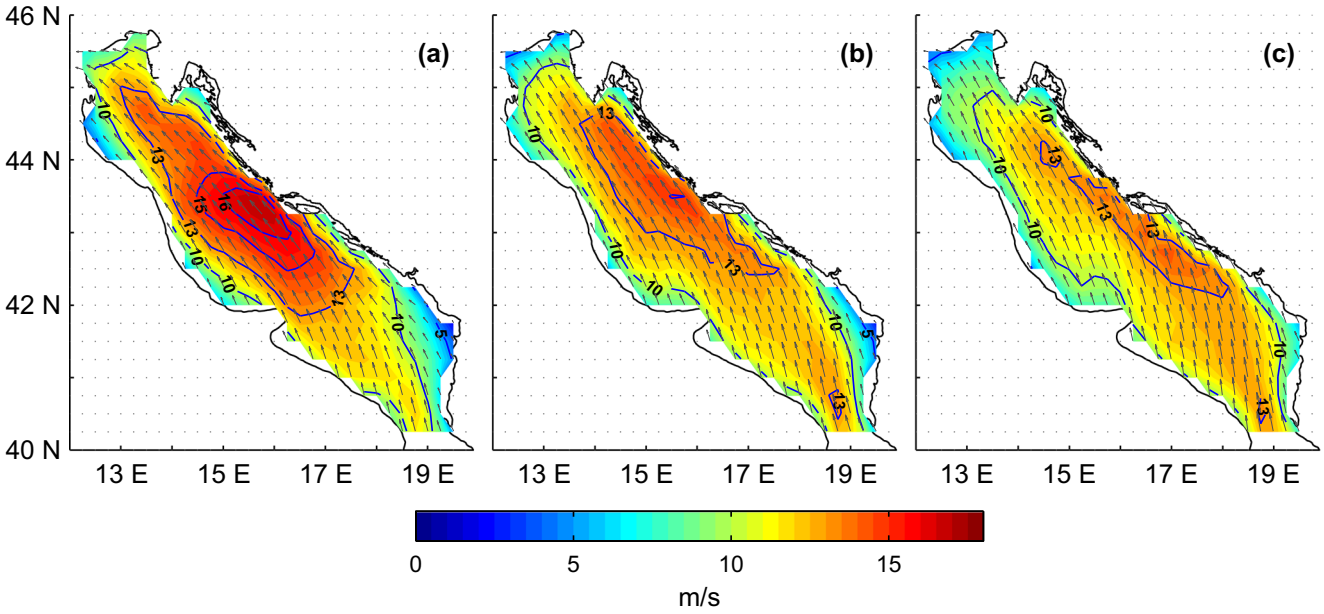

Fig. 5 Composite wind fields (ERA5) over the Adriatic for the three storm-surge types: the W type (**a**), O type (**b**), and E type (**c**)

given threshold. ALADIN52 resulted in 43% more events than ERA5, while the other regional models resulted in two (RCA4) or four (RegCM4) times more events.

Considering the proportion of realised episodes (Table 2, column 3), ERA5 expectedly yielded the best result, with almost every second wind episode being realised as high sea level. It should be emphasised again that strong wind, although dominantly contributing to sea-level change, is not the only component of the Adriatic floods. Closer inspection of Fig. 3. reveals that, for the unrealised events, the synoptic sea-level components are generally lower than for the realised ones, but they still overlap over a considerable range of values. This means that a number of the unrealised wind episodes are associated with exceptional storm surges but do not intersect with extreme sea levels because they coincided with a small planetary contribution. Because magnitudes of the planetary and the synoptic-scale components are not strongly related, as indicated by the dispersion of events in Fig. 3, our algorithm is not able to automatically detect only the realised ones. Additionally, it is possible that some of the wind fields are not reproduced properly, which may have reduced the percentage of realised episodes.

For regional climate models, the percentage of realised episodes (Table 2, column 3) is smaller and reflects two facts: (i) the larger number of wind episodes, due to the better resolution of the regional models, was relative to the constant number of actually realised (30) episodes in the considered period and (ii) RCMs do not intend to reproduce actual meteorological states. Comparing the percentages of realised and nonattributed episodes for the three RCMs, it follows that ALADIN52 is better than the other two. Concerning the frequency of events (Table 2, column 5), ALADIN52 and RCA4 give similar values, between 2.5 and 3.5 episodes per year, while RegCM4 results in twice as many. Hence, we can state that ALADIN52 and RCA4 reproduce the Adriatic southerly wind structures well, while RegCM4 is less skilled in this matter.

To examine the impact of model resolution on the results, velocities from RCM for evaluation runs were scaled by the ERA5/RCM ratio of monthly mean velocities over the 1984–2010 interval. Monthly mean velocities from ALADIN52 closely agree with ERA5 (not shown). The RCA4 values agree well in winter, while they deviate in summer. However, the RegCM4 monthly velocities differ significantly from the other models, especially during cold season when the extreme events are most frequent. RegCM4, although with higher wind speeds than in other two RCMs, followed the annual cycle comparable to ALADIN52 with distinct summer minimum and winter maximum in wind speeds. The scaled

Table 2 Datasets with number of extracted wind episodes in the evaluation interval (1984–2010). Realised wind episodes are expressed relative to the total number of wind episodes. Nonattributed sea-level episodes are expressed in relation to the number of actual sea-level episodes in the period of 1984–2010 (30 events). The yearly frequency of extracted wind episodes is given in the last column

Dataset	Number of episodes	Realised (%)	Nonattributed (%)	Frequency (year^{-1})
ERA5	49	45	27	1.8
ALADIN52	70	30	30	2.6
RCA4	94	16	50	3.5
RegCM4	195	5	67	7.2

wind fields from ALADIN52 and from RCA4 did not provide substantially different results than the original fields—the frequency of events became somewhat closer to the ERA5 frequency (2.1 events per year for both models), but the efficiency of the detection algorithm (percentages of the realised and the nonattributed events) did not improve. However, the scaled RegCM4 fields yielded a very small number of flooding episodes (0.30 events per year) and totally failed to reproduce the actual events (all the extracted episodes were unrealised). Obviously, this version of the RegCM4 model and set of simulations have strong limitations when it comes to storm-surge winds, and this fact should be taken into account when interpreting results and while planning future model application over the Adriatic region.

Climate statistics of the both reanalysis and historically driven RCM can be compared over the common period of all available input datasets, i.e. 1984–2000. Over this period, atmosphere-driven RCMs ingested sea-surface temperature and lateral boundary conditions from the ERA-Interim in the evaluation mode, and same quantities from the coupled GCMs in the historical mode. Nevertheless, the concentrations of the most important greenhouse gases were comparable in both modes of simulation. With this approach, models show similar climatology in terms of the frequency and intensity medians. For models ALADIN52, RCA4, and RegCM4, frequency medians in the evaluation runs are 2, 3, and 7 year^{-1} respectively, while the intensity medians are 11.9, 12.5, and 13.1 m/s. At the same time, in the historical simulations, we find comparable values of 5, 4.2, and 9.5 year^{-1} for the frequency, and 12.2, 12.3, and 13.4 m/s for the intensity (here, ALADIN52 historical values are associated with only single GCM, while values for other two RCMs are averaged over the ensemble of the GCM forced simulations). In addition, when evaluation runs are compared with the specific GCM run, the statistically significant differences are found in 3 out of 10 comparisons of the frequency, and only in 2 out of 10 cases when comparing the intensity.

4.3 Historical vs. future simulations

Here, we present the frequency, intensity, seasonal cycle, and type of the Adriatic southerly wind episodes (type W/E depending on whether they cause stronger sea-level response along the western or eastern coastline) in present and future climates. Two climate scenarios, moderate emission RCP4.5 and strong emission RCP8.5, were examined, as well as two future intervals—middle (2041–2070) and end (2071–2100) of the twenty-first century. The present climate estimations were based on historical simulations with data from 1971–2000. The analysis was carried out for all episodes together and then according to the episode types.

Considering the wind frequency for the three models in the present climate (Fig. 6, left), it is evident that there are differences in the model's own climatology. In RegCM4 simulations, episodes occur twice as often and with a much wider range of values. Models ALADIN52 and RCA4 are consistent and range from 3 to 6 events per year, while the frequency in RegCM4 ranges between 6 and 12. Simulations with initial and boundary conditions from the global model HadGEM2-ES differ from the rest of the set in most cases. Visual comparison of the present and future periods suggests minor differences between these climates. This was examined with the WMW test, which was applied to test the significance of the obtained differences—seven simulations, carried out with ALADIN52 and RCA4 (mostly for the end of the twenty-first century), deviated significantly from those in the present climate. An additional check was made through the climate change score *PCC* (*PCC* = 1-*PSS*, where *PSS* is the *Perkins skill score*), available in the Supplementary Materials (Table S1). On the basis of this statistical measure, a small (< 0.3) or moderate (0.3–0.50) probability for a change of wind frequency may be expected. These results suggest an increase in the number of events. However, if we consider that our dataset is large (32 projections) and that only a small percentage of simulations (22%) exhibited a significant change, then we can expect only minor variations in the number of intense wind episodes, under both scenarios, at the end of the twenty-first century.

Figure 7 shows spatial averages of wind velocities during extracted episodes. The models ALADIN52 and RCA4 generally give very close values, slightly more than 12 m/s, while RegCM4 exceeds this amount by less than 10%. Velocity ranges in RegCM4 simulations are wider than in the other two models, which is true for all of the studied intervals. In the future climate, wind velocities will not change significantly regardless of the future climate scenario. The WMW test showed that only two projections deviate from the present climate: RCA4 suggests a slight decrease, while RegCM4 indicates an increase of values. Hence, we can state that the wind velocity of intense episodes that favour flooding of the Adriatic coastlines will not change significantly in the future climate regardless of the scenario or time interval. This was confirmed by the corresponding *PCC*, whose values were low and did not exceed 0.18 (Table S2 in the Supplementary Materials).

Seasonal cycles in the number of southerly wind episodes in all simulations (Fig. 8) follow the expected pattern—the majority of events occur in the cold season when the passage of Mediterranean cyclones is frequent over the Adriatic. The most active month commonly falls between November and February. Amplitudes of the annual cycle are comparable in most simulations, and only those forced with the HadGEM1-ES global model diverge in some cases. Visual inspection of amplitudes and phases of the seasonal cycle does not give an indication of any change. Additionally, there are no obvious differences between the climate scenarios, nor between the

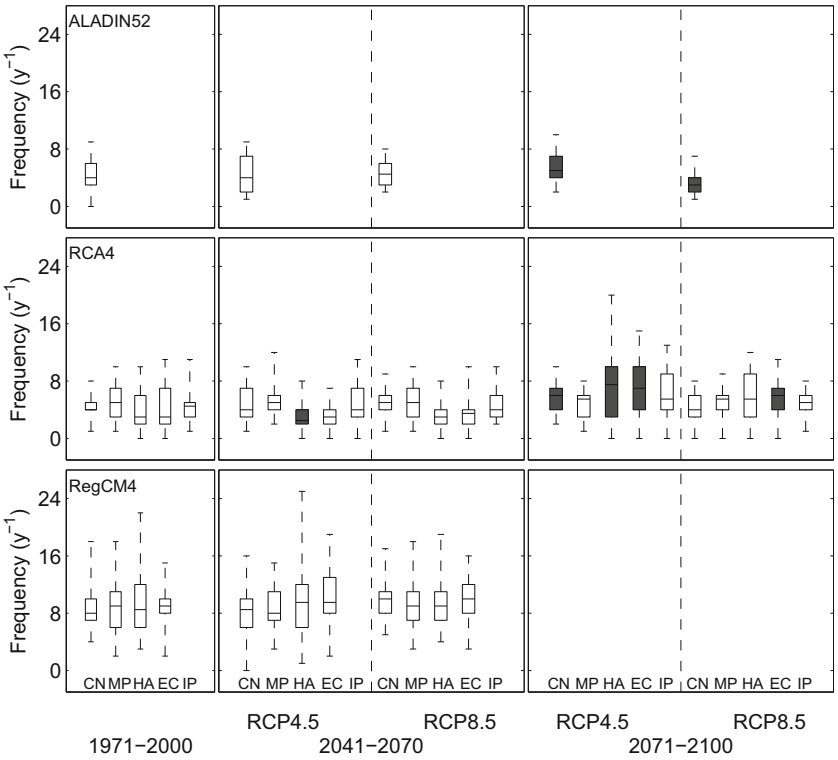

Fig. 6 Distribution of wind frequency for simulations by three RCMs in present and future climates. Filled symbols denote simulations in future scenarios that significantly differ (95% significance level) from those in the historical period. At the bottom are shown GCMs from which boundary and initial conditions were taken: CNRM-CM5 (CN), MPI-ESM-LR/MR (MP), HadGEM2-ES (HA), EC-EARTH (EC), and IPSL-CM5 (IP). In the box plot, the lowest and highest marks indicate the minimum and maximum values; in the box, the central mark indicates the median, and the bottom and top edges give the 25th and 75th percentiles, respectively

two future intervals. Here, formal testing was not done due to the small number of episodes in some months, but it is also unlikely that variations of the seasonal cycle would be significant considering the results for the other wind features.

Changes in the spatial structure of the wind fields that are responsible for extreme storm-surge events can be examined by studying characteristics of the wind field types that were identified in Sect. 3.3. Redistribution among the types would

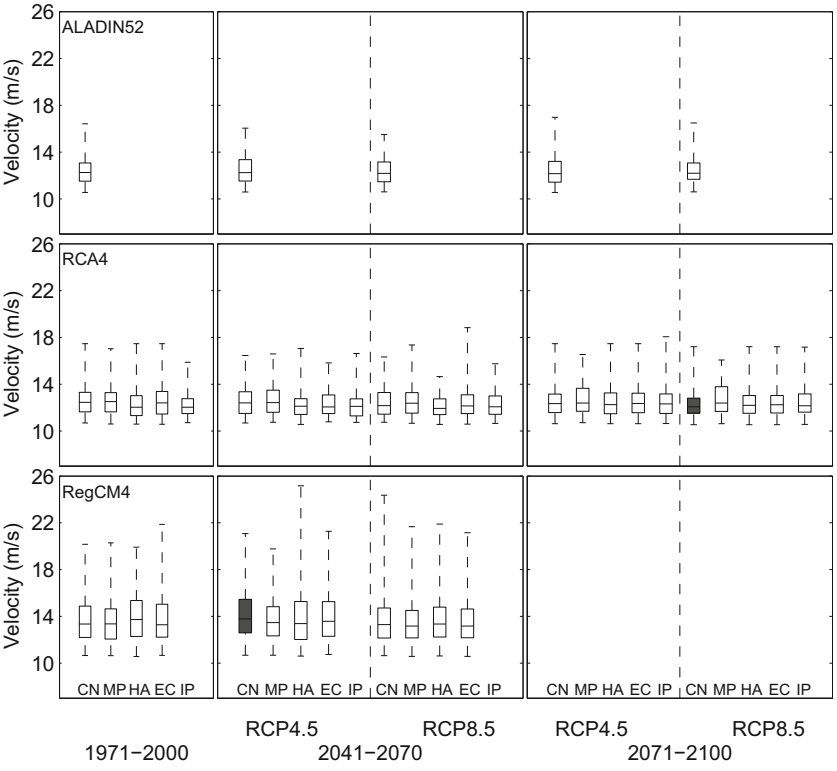

Fig. 7 Same as in Fig. 6 but for wind velocity

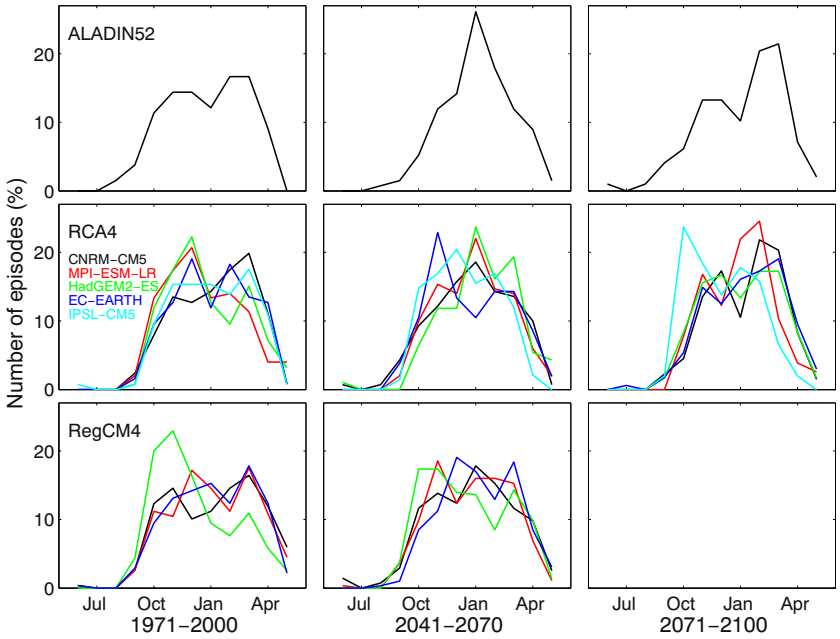

Fig. 8 Annual cycle of number of wind episodes for simulations with three RCMs forced with different global climate models (indicated with colours) in present and future climates. The results are shown for the extreme climate scenario RCP8.5, while those for RCP4.5 can be found in the Supplementary Materials (Fig. S2)

indicate a change of large spatial scale because different wind structures above the Adriatic are induced by cyclones of different intensity and position above the Mediterranean region (Međugorac et al. 2018). Distribution of the wind field types obtained from RCM simulations for the present-day climate is as expected—most episodes were classified as an ordinary type of wind field (~ 45%), while the rest were categorised, almost equally, as E or W type. Runs performed with RCA4 (IPSL-CM5) and RegCM4 (HadGEM2-ES) yielded the three wind types in similar proportions. This confirms that the selected regional climate models, ALADIN52, RCA4, and RegCM4, are skilled in reproduction of southerly wind fields over the Adriatic. Since the marginal wind types induce specific sea-level responses in the Adriatic, which in turn dictate which coastline will be more exposed to flooding, only results for W and E types will be given.

Presently, the frequency of the two marginal types (W and E) is similar, with slightly higher values for the W type (Figs. 9 and 10, left). All three models are in agreement on this, with RegCM4 giving higher frequencies for both wind types. The W and E events occur approximately 1–2 times a year (almost three times a year in the case of RegCM4). Furthermore, frequency distributions for the middle and the end of the twenty-first century (Figs. 9 and 10, middle and right panel) are similar to those in the present climate, and there are no indications that the number of one type will increase on account of the other. According to the WMW test, the difference between future and present climates, for the W type of wind fields, is significant in only two simulations. These suggest more frequent flooding of the western coast in the future. A similar result was obtained for E-type fields—only one simulation implies a significant increase in the frequency of floods along the eastern coast (by one episode per year). Hence, only a small percentage of realisations (6% in the case of the W and 3% in the case of the E type) suggest a significant change. Analysis of *PCC* gives similar results. Values of *PCC* are smaller than 0.30, except in two simulations of the W field and two of the E field, where *PCC* does not exceed 0.37 (Tables S3 and S4 in the Supplementary Materials). Thus, the probability that, in a future climate, the frequency of flood-favouring wind fields will change is small, for W- as well as for E-type wind field.

Changes in the intensity of the W and E types of wind fields were also examined (Figs. 11 and 12). In the present climate, the two wind types have similar spatially averaged velocities of approximately 12.4 m/s. For RegCM4, velocity medians are slightly higher (13.8 m/s) with much wider distributions of magnitudes (the velocity exceeds 22 m/s in some cases). For the future climate (middle and right panels of Figs. 11 and 12), there is no evidence that the types might intensify or weaken. Only one simulation for each type (in both cases, it is RegCM4 forced with CNRM-CM5) gives a significant increase of velocity. Corresponding values of *PCC* are low (in two runs for W type and one run for E type, $PCC \geq 0.30$), suggesting a low probability of increasing/decreasing wind velocity for both types of wind field (Tables S5 and S6 in the Supplementary Materials).

5 Discussion

Central point in the analysis was to create the algorithm which would detect extreme sea-level events on the basis of hourly wind fields from ERA5 reanalysis. The algorithm was tested

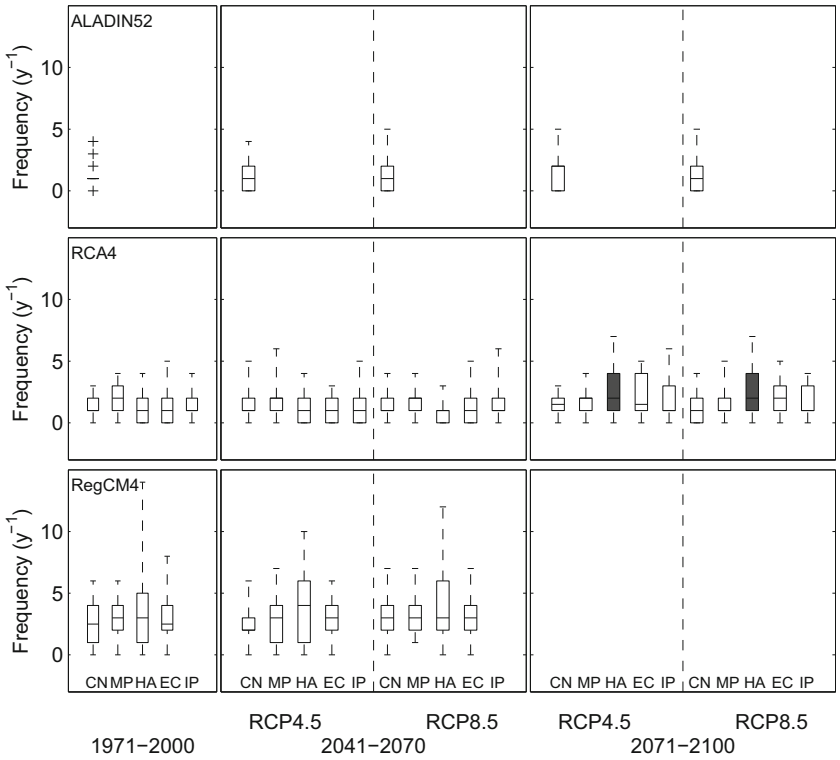

Fig. 9 Frequency of wind episodes of the W type. Details as in Fig. 6

against the observed sea-level events in the northern Adriatic. More than 70% of actual events were detected. However, 54% of the extracted wind episodes were not realised. Nevertheless, we may consider the algorithm fairly efficient, having in mind that we are detecting only the major contribution, which acts simultaneously with the other processes.

Considering unrealised episodes, on several occasions, synoptic sea-level components were considerably high (about

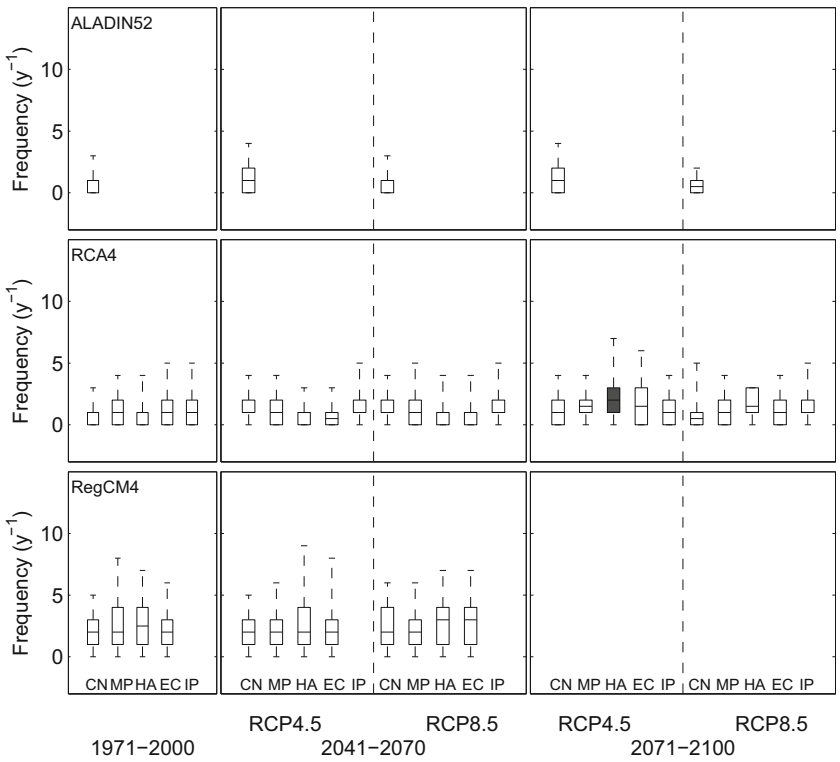

Fig. 10 Frequency of wind episodes of the E type. Details as in Fig. 6

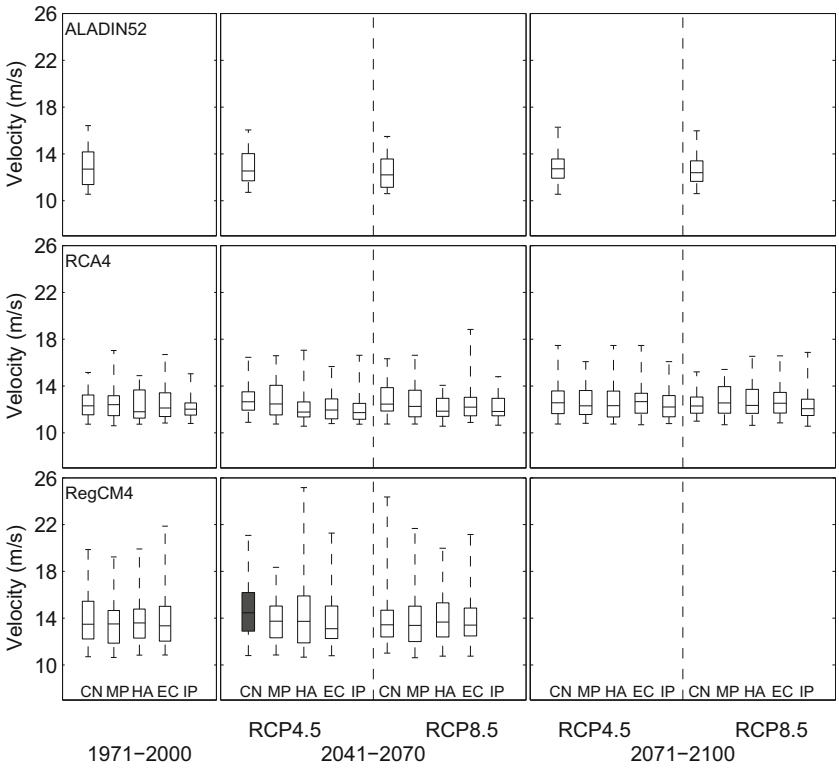

Fig. 11 Velocity during wind episodes of the W type. Details as in Fig. 6

50 cm), but events were not realised as exceptional sea levels because amplitudes of concurrent planetary components were low. On the other hand, on two occasions (nonattributed episodes Z10 and Z17), the synoptic sea-level component was extremely high (76 cm and 62 cm, respectively), but the algorithm did not detect these extreme events. Closer inspection revealed that during these two events, strong wind was blowing, exceeding mean value of 10.50 m/s in several consecutive

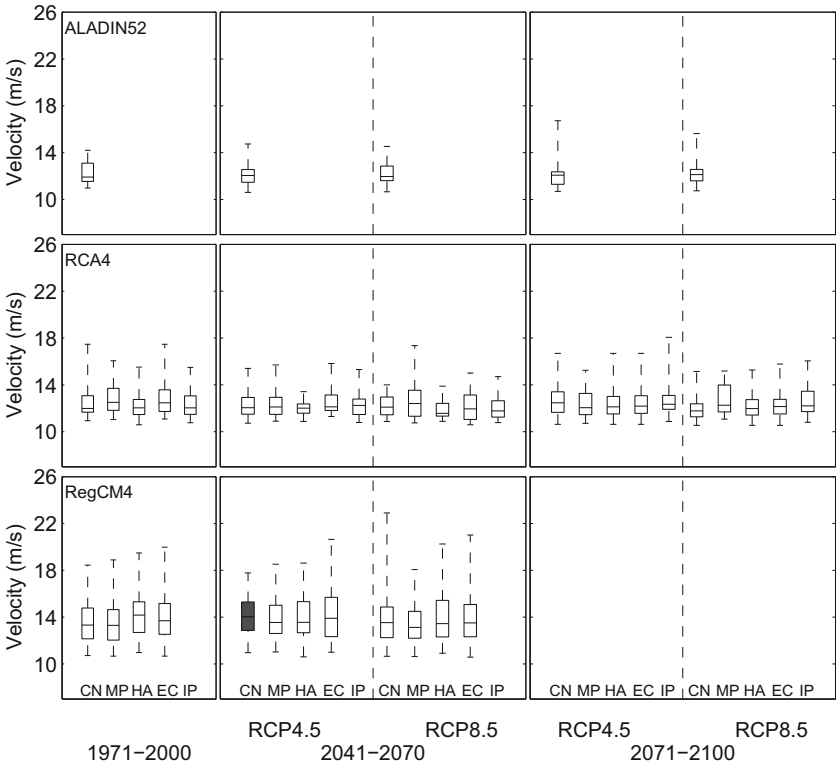

Fig. 12 Velocity during wind episodes of the E type. Details as in Fig. 6

intervals, but from NW or SW direction over the greater portion of the basin. Moreover, episode 17 was also influenced by previously triggered seiche which positively overlapped with newly induced storm surge and additionally raised sea level. Evidently, in order to capture all flooding events, a wider range of wind directions should be taken into account. However, this brings in greater number of the unrealised events, so a compromise had to be made to obtain the best ratio of the realised to unrealised and nonattributed events.

The performance of the wind-based algorithm for detection of flooding events is further supported by the distribution of the established sea-level slopes (Fig. 4), which is similar to the one for the actual sea-level events. The discrepancies may arise from excluding/allowing certain forms of wind but also from the way that sea level was associated with every wind episode. It should be borne in mind that the sea-level peaks occur after the wind maxima with different time legs. Because we limited this time interval to a maximum of 12 h, it is possible that in some wind episodes, we have overestimated/underestimated the actual sea-level slope.

The analysed regional climate models are not equally successful in reproducing flood-threatening wind fields, and here, ALADIN52 is superior to the other two. Better performance of ALADIN52 is related in part to the size and location of its domain: ALADIN52 covers a wider Mediterranean area (as set in the Med-CORDEX protocol), while the domains of RCA4 and RegCM4 spread over the whole of Europe (as set in the EURO-CORDEX protocol). Because the domain size affects the temporal correlation in circulation patterns, the use of larger domains may lead to smaller temporal correlations (Leduc and Laprise 2009), and thus it is understandable that RCA4 and RegCM4 are generally less efficient in reproducing the temporal sequence of specific meteorological situations. In addition, smaller domains allow greater impact of boundary conditions (Žagar et al. 2013), which can raise the skill of the RCM when forced by the reanalysis with the correct sequence of the synoptic weather patterns. The relation between domain size and wind field quality, as discussed here, could have been tested had the ALADIN52 subdaily fields been available for a greater domain. However, at the time of writing, only daily simulations were accessible for the wider European domain (from the CORDEX database). RegCM4 showed large deviations from the other two models. Comparing the frequencies based on the original (7.2 year^{-1}) and scaled (0.3 year^{-1}) wind fields, one can conclude that RegCM4 allows the development of a stronger wind than the other two models, but its simulated duration is shorter. This limitation may come from the surface friction formulation and planetary boundary layer scheme implemented in the model, but focused model sensitivity studies are needed to address this issue/problem.

The analysis showed that features of wind episodes favouring flooding of the northern Adriatic coast probably will not change in future climates, supported by the results of all three RCMs. The probability that the frequency, intensity, seasonal cycle, and spatial structure of potentially dangerous wind fields will change in future climates is small. Simulations obtained by using the three regional climate models, forced with several different global models, gave qualitatively the same results. The obtained result does not depend on the climate scenario, future period, or regional or global climate model. This is in line with the two previous studies on the topic (Lionello et al. 2012b; Mel et al. 2013), although these were based on a single model, so the results could had been influenced by the outliers or by the selection of the specific scenario–GCM–RCM chain of assumptions. Given the well-known wide spread of climate simulations (IPCC 2013), the conclusions reached now, on the basis of a number of different criteria, have substantial reliability. Denamiel et al. (2020) obtained somewhat different results. Using the pseudo–global warming method on twelve selected storm surges observed at stations Venice and Trieste during 1979–2019, they obtained a notable decrease of their amplitude under the climate scenarios RCP4.5 and RCP8.5 expected during 2060–2100. However, the disagreement might come from the fact that Denamiel et al. (2020) analysed storm surges related to severe wave storms, and these are, in most cases, caused by cyclones of different characteristics than those that generate severe storm surges (Lionello et al. 2012a).

Although extremes in the near-surface temperature and precipitation amounts over the Mediterranean are expected to intensify during the twenty-first century, the same RCM–GCM simulations do not show a clear impact on the near-surface winds responsible for flooding of the Adriatic coasts. Numerous studies (e.g. Giorgi and Lionello 2008; Gualdi et al. 2013; Adloff et al. 2015) have shown that the mean sea-level pressure (MSLP) will increase over large parts of the Mediterranean, consistent with the shift of trajectories of the Atlantic cyclones to the north, suggesting an increase of anticyclonic activity. Therefore, we assumed that these changes would impact the occurrence of the Adriatic southerly wind episodes that are caused by Mediterranean cyclones. One of the reasons for the absence of a clear sign of changes in storm-surge activity may be the seasonal modulation of the climate change signal. According to Giorgi and Lionello (2008), the expected MSLP changes over the Mediterranean exhibit a strong seasonal dependence, and they are most pronounced during summer. Since Mediterranean cyclones causing extreme storm surges in the Adriatic are mostly generated in late autumn and winter, it is likely that they are not sensitive to the abovementioned changes. This topic deserves a detailed analysis in a future study.

It should be repeatedly stressed that the Adriatic floods are the result of combined effects of several processes and that we here analysed the meteorological background of only the dominant one—storm surge. As presented in Fig. 3, another important component of floods is the planetary component of

sea level, which can contribute to these events with more than 40 cm. Closer inspection of the sea level during the wind episodes revealed that in several cases, difference of the planetary component between Venice and Bakar was considerable (up to 10 cm). This indicates that some other process, other than adjustment to planetary atmospheric waves, may have affected sea level at low frequencies. De Zolt et al. (2006) reported that in preceding months of the 1966 flood, precipitation over the eastern Alpine and pre-Alpine areas was persistent and intensive, which made surrounding rivers reach exceptional discharge values. Prolonged intervals of very large river inflow could reflect on planetary sea-level component in an area like the Venice lagoon, but for reliable conclusion, a detailed analysis should be carried out.

In addition, local seiches and wave setup, both driven by wind, can substantially affect the water level along the coastline. In this study, using hourly sea-level data, the first process was filtered out (e.g. the period of the first mode of the Bakar Bay seiches is 20 min). Alternately, using data from stations placed at sites protected from direct impact by wind waves (the Bakar station is in the bay sheltered by the chain of islands, and the Venice station is in the lagoon), we reduced the contribution of the wave setup (Bowen et al. 1968). To estimate the exact wave setup effect on the water level, it is necessary to run a wave model, which is beyond the scope of this article, but some estimations can still be given and discussed. The strongest flood ever recorded at the Venice Punta Salute station occurred on 4 November 1966, when wind waves in the northern Adriatic were 8-m high; the wave setup at a location in front of Venice was estimated to be 15% of the total sea level reached at the site (De Zolt et al. 2006). No data for the wave setup in the lagoon were provided, but it can be assumed that the contribution was smaller. If we consider that on this occasion, the wind accumulated water up to almost 2 m in height at Venice Punta Salute, whereas considerably lower levels were reached during the events that we are analysing (Fig. 3), it is reasonable to assume that the wave setup effect in the studied episodes was notably lower than 15% and is incorporated in the synoptic-scale component.

6 Summary and conclusions

In this research, we analysed the impact of climate change on the wind fields responsible for the Adriatic storm surges. The dataset consisted of sea levels measured at Venice and Bakar (1984–2014), the corresponding ERA5 wind fields, and wind simulations of three CORDEX RCMs (ALADIN52, RCA4, and RegCM4) forced with several GCMs. For future climate conditions, we considered two scenarios (RCP4.5 and RCP8.5) in two 30-year intervals—the middle (2041–2070) and end (2071–2100) of the twenty-first century. The strategy was to create algorithms that will reliably extract wind structures that are responsible for extreme storm surges using measured sea levels and ERA5 wind fields and then apply the same algorithms to study these structures in climate simulations. The goal was (i) to evaluate the selected regional climate models in reproduction of southerly wind episodes over the Adriatic and (ii) to analyse the effect of climate change on these events.

Considering the results for the evaluation period (simulations forced with ERA-Interim), the models ALADIN52 and RCA4 reproduced well exact meteorological situations, while RegCM4 was less successful. In the present climate conditions (historical period), the three RCMs followed the expected seasonal cycle—a larger number of southerly wind structures occurred during the cold season. For the frequency and intensity of these events, ALADIN52 and RCA4 gave consistent values, while values from RegCM4 are somewhat higher and spread over a wider range of values. Analysis of wind features in the present and future scenarios revealed that there is a small probability that climate change will have any effect on this type of event. More specifically, the frequency, intensity, seasonal cycle, and spatial structure of the southerly wind in the twenty-first century are likely to remain the same as those in the current climate. The study did not find evidence (based on the type of wind fields) that one coastline, the western or the eastern, will be exposed to greater risk than it is today. These results are independent of all the considered criteria—they do not depend on the used model, regional or global, greenhouse gas scenario, or upcoming time interval. The conclusion is based on a large ensemble of simulations, which provides it substantial reliability.

The Adriatic floods are the outcome of the combined effect of several processes on different spatial and temporal scales, where the storm surges play a dominant role. Here, we examined meteorological conditions of storm surges only, but to achieve a full picture of future atmospheric forcing of floods, it is necessary to study meteorological backgrounds of the Adriatic-wide seiche and planetary component. This is an appealing topic for upcoming research. In addition, the presented type of analysis should be repeated on larger ensembles of non-hydrostatic and coupled atmosphere–ocean regional climate simulations, whose development and availability are expected in the near future.

Acknowledgements Many thanks to Hrvoje Mihanović (Institute of Fisheries and Oceanography, Split) for his help with Matlab scripts and fruitful discussion. The EURO-CORDEX data used in this work were obtained from the Earth System Grid Federation server (https://esgfdata.dkrz.de/projects/esgf-dkrz/). The Med-CORDEX data used in this work were obtained from the Med-CORDEX server (www.medcordex.eu). We are grateful to all EURO-CORDEX and Med-CORDEX modelling groups that performed the simulations and made their data available. We acknowledge the World Climate Research Programme's Working Group on Coupled Modelling, which is responsible for CMIP, and we thank the climate modelling groups for producing and making available their model output. And last but not least, many thanks to anonymous reviewer for his/her helpful comments and suggestions which made this work better.

Funding This work was supported by the Croatian Science Foundation under the projects CARE (grant number HRZZ-IP-2013-11-2831) and MAUD (grant number HRZZ-IP-2018-01-9849). RegCM4 simulations analysed in this study were performed as a part of the Croatian Ministry of Environment and Energy project "Strengthening the Capacity of the Ministry of Environment and Energy for Climate Change Adaptation and development of the Draft Strategy for Climate Change Adaptation (Contract number: TF/HR/P3-M1-O1-010)" funded by the EU Transition Facility.

Appendix 1. Estimation of sea-level trends and difference between two locations

Here, we describe the method used to determine non-atmospherically related sea-level trends in Venice and Bakar. Generally, different processes can cause changes of the mean sea level that are recorded at a location by a tide gauge: direct atmospheric forcing, thermohaline processes, mass changes, and crustal movements. Here, it was necessary to separate the sea-level trend caused by direct atmospheric forcing from that caused by other processes. To do so, we use the fact that sea-level anomalies, i.e. departures of sea level from the mean seasonal cycle, are highly correlated with respective anomalies of air pressure (Orlić and Pasarić 2000). Parameters of linear regression between the two time series are applied to air pressure anomalies to obtain the sea-level variability due to direct atmospheric forcing. Once this part is subtracted from the observed sea-level data, the residual time series exhibits a trend that is presumably related to the latter three processes.

The analysis was conducted on time series of monthly mean values of sea level (z_m) and air pressure (p_m). These were used to calculate the mean seasonal cycles of sea level (z_s) and air pressure (p_s) as long-term averages of values for each month and to obtain the respective anomalies ($z_a = z_m - z_s$; $p_a = p_m - p_s$). Linear regression between sea-level anomalies and air pressure anomalies, $z_a = A \cdot p_a + \varepsilon$, where ε is the error term, yields an adjustment of sea level in the northern Adriatic ($A = -2.15$ cm/hPa at Bakar, $A = -2.07$ cm/hPa at Venice, with correlation coefficient $r = 0.84$ for Bakar, $r = 0.81$ for Venice) that is two times stronger than the inverse barometer effect. The overshoot is due to wind forcing that acts coherently and in the same sense as the air pressure forcing (Pasarić et al. 2000). The non-seasonal sea-level variability induced by air pressure and wind forcing, $z_p = A \cdot p_a$, and subsequently the residual time series, $z_r = z_a - z_p$, that is related to thermohaline forcing, global mass change, and vertical land movements is evaluated to determine the trend in sea level that is not imposed by the direct atmospheric forcing. Time series of annual mean sea level, the atmospherically induced sea level, and the residual part with the respective linear trends (a, a_p, a_r) are shown in Fig. 13. The linear trends with their uncertainty intervals were determined using Bayesian statistics to take into account autocorrelation within the time series (Orlić et al. 2018). The sea-level trends are much larger than those reported for the 1960–2000 interval (Marcos and Tsimplis 2008). They reflect the fact that over the last two decades, the sea-level rise in the Adriatic and elsewhere in the Mediterranean has been accelerating (Orlić et al. 2018). The trend in Venice is more consistent with the values for the

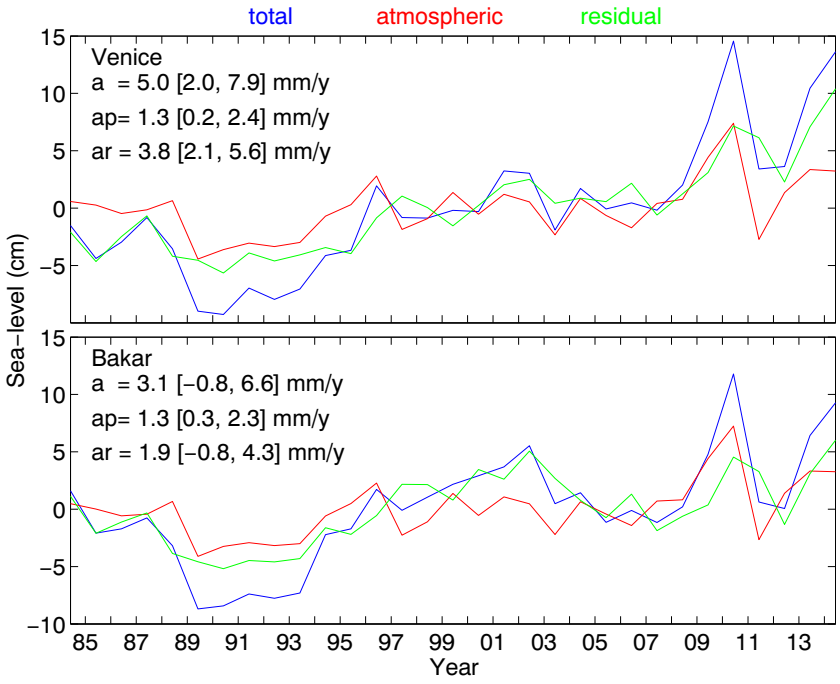

Fig. 13 Time series of annual mean sea level at Venice and Bakar: total sea level, variability induced by direct atmospheric forcing, and the residual sea level. Also shown are the respective trends (a, a_p, a_r), with the 90% credible intervals in brackets

1993–2015 period (Vignudelli et al. 2019). Furthermore, the total sea-level rise (a), as well as the rise of the residual sea level (a_r), is much higher in Venice than in Bakar. The difference can partly be attributed to the land subsidence in Venice that is still ongoing at a rate of some 1.0 ± 0.7 mm/year (Tosi et al. 2013). However, a detailed analysis of sea-level trends is beyond the scope of this study.

References

Adloff F, Somot S, Sevault F et al (2015) Mediterranean Sea response to climate change in an ensemble of twenty first century scenarios. Clim Dyn 45(9-10):2775–2802. https://doi.org/10.1007/s00382-015-2507-3

AMGI (2018). Press release. https://www.pmf.unizg.hr/geof?@=1kzz9.

Bajo M, Umgiesser G (2010) Storm surge forecast through a combination of dynamic and neural network models. Ocean Model 33(1-2):1–9. https://doi.org/10.1016/j.ocemod.2009.12.007

Bajo M, Zampato L, Umgiesser G, Cucco A, Canestrelli P (2007) A finite element operational model for storm surge prediction in Venice. Estuar Coast Shelf Sci 75(1-2):236–249. https://doi.org/10.1016/j.ecss.2007.02.025

Bajo M, Međugorac I, Umgiesser G, Orlić M (2019) Storm surge and seiche modelling in the Adriatic Sea and the impact of data assimilation. Q J R Meteorol Soc 145(722):2070–2084. https://doi.org/10.1002/qj.3544

Belmonte Rivas M, Stoffelen A (2019) Characterizing ERA-Interim and ERA5 surface wind biases using ASCAT. Ocean Sci 15:831–852. https://doi.org/10.5194/os-15-831-2019

Belušić Vozila A, Güttler I, Ahrens B, Obermann-Hellhund A, Telišman Prtenjak M (2019) Wind over the Adriatic region in CORDEX climate change scenarios. J Geophys Res-Atmos 124(1):110–130. https://doi.org/10.1029/2018JD028552

Belušić A, Prtenjak Telišman M, Güttler I, Ban N, Leutwyler D, Schär C (2018) Near-surface wind variability over the broader Adriatic region: insights from an ensemble of regional climate models. Clim Dyn 50(11-12):4455–4480. https://doi.org/10.1007/s00382-017-3885-5

Bowen AJ, Inman DL, Simmons VP (1968) Wave set-down and set-up. J Geophys Res 73(8):2569–2577

Copernicus Climate Change Service (C3S) (2017) ERA5: Fifth generation of ECMWF atmospheric reanalyses of the global climate. Copernicus Climate Change Service Climate Data Store (CDS) 15(2):2020 https://cds.climate.copernicus.eu/cdsapp#!/home

Cerovečki I, Orlić M, Hendershott MC (1997) Adriatic seiche decay and energy loss to the Mediterranean. Deep-Sea Res Pt I 44(12):2007–2029. https://doi.org/10.1016/S0967-0637(97)00056-3

Colin J, Déqué M, Radu R, Somot S (2010) Sensitivity study of heavy precipitation in limited area model climate simulations: influence of the size of the domain and the use of the spectral nudging technique. Tellus A 62(5):591–604. https://doi.org/10.1111/j.1600-0870.2010.00467.x

De Zolt S, Lionello P, Malguzzi P, Nuhu A, Tomasin A (2006) The disastrous storm of 4 November 1966 on Italy. Nat Hazard Earth Sys 6:861–879

Dee DP, Uppala SM, Simmons AJ et al (2011) The ERA-interim reanalysis: configuration and performance of the data assimilation system. Q J Roy Meteor Soc 137:553–597. https://doi.org/10.1002/qj.828

Denamiel C, Pranić P, Quentin F, Mihanović H, Vilibić V (2020) Pseudo-global warming projections of extreme wave storms in complex coastal regions: the case of the Adriatic Sea. https://doi.org/10.1007/s00382-020-05397-x

Dullaart JCM, Muis S, Bloemendaal N et al (2020) Advancing global storm surge modelling using the new ERA5 climate reanalysis. Clim Dyn 54:1007–1021. https://doi.org/10.1007/s00382-019-05044-0

Dutour Sikirić M, Janeković I, Tomažić I, Kuzmić M, Roland A (2015) Comparison of ALADIN and IFS model wind speeds over the Adriatic. Acta Adriat 6(1):67–82

Fisz M (1963) Probability theory and mathematical statistics. John Wiley & Sons Ltd, Malabar

Giorgi F, Lionello P (2008) Climate change projections for the Mediterranean region. Glob Planet Chang 63(2-3):90–104. https://doi.org/10.1016/j.gloplacha.2007.09.005

Giorgi F, Coppola E, Solmon F, Mariotti L, Sylla MB, Bi X, Elguindi N, Diro GT, Nair V, Giuliani G et al (2012) RegCM4: model description and preliminary tests over multiple CORDEX domains. Clim Res 52:7–29. https://doi.org/10.3354/cr01018

Godin G, Trotti L (1975) Trieste-water levels 1952–1971: a study of the tide, mean level, and seiche activity. Miscellaneous special publication 28. Department of the Environment, Fisheries and Marine Service, Ottawa

Gualdi S, Somot S, Li L et al (2013) The CIRCE simulations: regional climate change projections with realistic representation of the Mediterranean Sea. B Am Meteorol Soc 94(1):65–81. https://doi.org/10.1175/BAMS-D-11-00136.1

Hersbach H, Dee D (2016) ERA5 reanalysis is in production. ECMWF Newsletter 147(7)

Hersbach H, de Rosnay P, Bell B, Schepers D, Simmons A, Soci C, Abdalla S, Alonso Balmaseda M, Balsamo G, Bechtold P, Berrisford P, Bidlot J, de Boisséson E, Bonavita M, Browne P, Buizza R, Dahlgren P, Dee D, Dragani R, Diamantakis M, Flemming J, Forbes R, Geer A, Haiden T, Hólm E, Haimberger L, Hogan R, Horányi A, Janisková M, Laloyaux P, Lopez P, Muñoz-Sabater J, Peubey C, Radu R, Richardson D, Thépaut JN, Vitart F, Yang X, Zsótér E, Zuo H (2018) Operational global reanalysis: progress, future directions and synergies with NWP, ECMWF ERA Report Series 27. https://doi.org/10.21957/tkic6g3wm

Hersbach H, Bell B, Berrisford P, Horányi A, Sabater JM, Nicolas J, Radu R, Schepers D, Simmons A, Soci C, Dee D (2019) Global reanalysis: goodbye ERA-Interim, hello ERA5. ECMWF Newsletter 159:17–24. https://doi.org/10.21957/vf291hehd7

IPCC (2013) Climate change 2013: the physical science basis. In: Stocker TF, Qin D, Plattner G-K, Tignor M, Allen SK, Boschung J, Nauels A, Xia Y, Bex V, Midgley PM (eds) Contribution of working group I to the Fifth Assessment Report of the Intergovernmental Panel on Climate Change. Cambridge University Press, Cambridge, United Kingdom and New York http://www.ipcc.ch/report/ar5/

Jacob D, Petersen J, Eggert B et al (2014) EURO-CORDEX: new high-resolution climate change projections for European impact research. Reg Environ Chang 14(2):563–578. https://doi.org/10.1007/s10113-013-0499-2

Janeković I, Kuzmić M (2005) Numerical simulation of the Adriatic Sea principal tidal constituents. Ann Geophys 23:3207–3218. https://doi.org/10.5194/angeo-23-3207-2005

Kotlarski S, Keuler K, Christensen OB et al (2014) Regional climate modeling on European scales: a joint standard evaluation of the EURO-CORDEX RCM ensemble. Geosci Model Dev 7(4):1297–1333. https://doi.org/10.5194/gmd-7-1297-2014

Leduc M, Laprise R (2009) Regional climate model sensitivity to domain size. Clim Dyn 32(6):833–854. https://doi.org/10.1007/s00382-008-0400-z

Lionello P, Cavaleri L, Nissen KM, Pino C, Raicich F, Ulbrich U (2012a) Severe marine storms in the northern Adriatic: characteristics and trends. Phys Chem Earth 40(41):93–105. https://doi.org/10.1016/j.pce.2010.10.002

Lionello P, Galati MB, Elvini E (2012b) Extreme storm surge and wind wave climate scenario simulations at the Venetian littoral. Phys Chem Earth 40:86–92. https://doi.org/10.1016/j.pce.2010.04.001

Marcos M, Tsimplis MN (2008) Coastal sea level trends in Southern Europe. Geophys J Int 175:70–82. https://doi.org/10.1111/j.1365-246X.2008.03892.x

Marcos M, Jordà G, Gomis D, Pérez B (2011) Changes in storm surges in Southern Europe from a regional model under climate change scenarios. Glob Planet Chang 77(3-4):116–128. https://doi.org/10.1016/j.gloplacha.2011.04.002

Međugorac I, Pasarić M, Orlić M (2015) Severe flooding along the eastern Adriatic coast: the case of 1 December 2008. Ocean Dyn 65(6): 817–830. https://doi.org/10.1007/s10236-015-0835-9

Međugorac I, Pasarić M, Pasarić Z, Orlić M (2016) Two recent storm-surge episodes in the Adriatic. Int J Safety Sec Eng 6(3):589–596. https://doi.org/10.2495/SAFE-V6-N3-589-596

Međugorac I, Orlić M, Janeković I, Pasarić Z, Pasarić M (2018) Adriatic storm surges and related cross-basin sea-level slope. J Mar Syst 181: 79–90. https://doi.org/10.1016/j.jmarsys.2018.02.005

Mel R, Sterl A, Lionello P (2013) High resolution climate projection of storm surge at the Venetian coast. Nat Hazard Earth Sys 13(4): 1135–1142. https://doi.org/10.5194/nhess-13-1135-2013

Menendez M, García-Díez M, Fita L, Fernández J, Méndez FJ, Gutiérrez JM (2014) High-resolution sea wind hindcasts over the Mediterranean area. Clim Dyn 42(7-8):1857–1872. https://doi.org/10.1007/s00382-013-1912-8

Moss RH, Edmonds JA, Hibbard KA et al (2010) The next generation of scenarios for climate change research and assessment. Nature 463: 747–756. https://doi.org/10.1038/nature08823

Orlić M (1983) On the frictionless influence of planetary atmospheric waves on the Adriatic Sea level. J Phys Oceanogr 13:1301–1306

Orlić M, Pasarić M (2000) Sea-level changes and crustal movements recorded along the east Adriatic coast. Nuovo Cimento C 23(4): 351–364

Orlić M, Kuzmić M, Pasarić Z (1994) Response of the Adriatic Sea to the bora and sirocco forcing. Cont Shelf Res 14(1):91–116. https://doi.org/10.1016/0278-4343(94)90007-8

Orlić M, Pasarić M, Pasarić Z (2018) Mediterranean sea-level variability in the second half of the twentieth century: a Bayesian approach to closing the budget. *Pure Appl Geophys* 175:3973–3988. https://doi.org/10.1007/s00024-018-1974-y

Pasarić M, Orlić M (1992) Response of the Adriatic Sea level to the planetary-scale atmospheric forcing. Geogr Monog Ser 69:29–39. https://doi.org/10.1029/GM069p0029

Pasarić M, Orlić M (2001) Long-term meteorological preconditioning of the North Adriatic coastal floods. Cont Shelf Res 21:263–278. https://doi.org/10.1016/S0278-4343(00)00078-9

Pasarić M, Pasarić Z, Orlić M (2000) Response of the Adriatic sea level to the air pressure and wind forcing at low frequencies (0.01 – 0.1 cpd). J Geophys Res 105:11423–11439. https://doi.org/10.1029/2000JC900023

Pawlowicz R, Beardsley B, Lentz S (2002) Classical tidal harmonic analysis including error estimates in MATLAB using T_TIDE. Comput Geosci 28:929–937. https://doi.org/10.1016/S0098-3004(02)00013-4

Perkins SE, Pitman AJ, Holbrook NJ, McAneney J (2007) Evaluation of the AR4 climate models' simulated daily maximum temperature, minimum temperature, and precipitation over Australia using probability density functions. J Clim 20(17):4356–4376

Porcu F, Aragão L, Aguzzi M, Valentini A, Debele S, Kumar P, Loupis M, Montesarchio M, Mercogliano P, Di Sabatino S (2020) Extreme wave events attribution using ERA5 datasets for storm-surge studies in the northern Adriatic Seae. EGU General Assembly 2020. https://doi.org/10.5194/egusphere-egu2020-19443

Raicich F, Orlić M, Vilibić I, Malačič V (1999) A case study of the Adriatic seiches (December 1997). Nuovo Cimento C 22(5):715–526

Robinson A, Tomasin A, Artegiani A (1973) Flooding of Venice: phenomenology and prediction of the Adriatic storm surge. Q J Roy Meteor Soc 99(422):688–692. https://doi.org/10.1002/qj.49709942210

Ruti PM, Somot S, Giorgi F et al (2016) MED-CORDEX initiative for Mediterranean climate studies. B Am Meteorol Soc 97(7):1187–1208. https://doi.org/10.1175/BAMS-D-14-00176.1

Samuelsson P, Jones CG, Willén U, Ullerstig A, Gollvik S, Hansson ULF, Jansson E, Kjellstro MC, Nikulin G, Wyser K (2011) The Rossby Centre regional climate model RCA3: model description and performance. Tellus A 63(1):4–23. https://doi.org/10.1111/j.1600-0870.2010.00478.x

Taylor KE, Stouffer RJ, Meehl GA (2012) An overview of CMIP5 and the experiment design. B Am Meteorol Soc 93(4):485–498. https://doi.org/10.1175/BAMS-D-11-00094.1

Tosi L, Teatini P, Strozzi T (2013) Natural versus anthropogenic subsidence of Venice. Sci Rep-UK 3:2710. https://doi.org/10.1038/srep02710

Trigo IF, Davies TD (2002) Meteorological conditions associated with sea surges in Venice: a 40 year climatology. Int J Climatol 22(7): 787–803. https://doi.org/10.1002/joc.719

Vignudelli S, De Biasio F, Scozzari A, Zecchetto S, Papa A (2019) Sea level trends and variability in the Adriatic Sea and around Venice. In: International Association of Geodesy Symposia. Springer, Berlin, Heidelberg. https://doi.org/10.1007/1345_2018_51

Vilibić I, Šepić J, Pasarić M, Orlić M (2017) The Adriatic Sea: a long-standing laboratory for sea level studies. Pure Appl Geophys 174(10):3765–3811. https://doi.org/10.1007/s00024-017-1625-8

Žagar N, Honzak L, Žabkar R, Skok G, Rakovec J, Ceglar A (2013) Uncertainties in a regional climate model in the midlatitudes due to the nesting technique and the domain size. J Geophys Res-Atmos 118(12):6189–6199. https://doi.org/10.1002/jgrd.50525